EUROPEAN ORGANIZATION FOR NUCLEAR RESEARCH

L3 Note 2566
June 28, 2000.

$\Lambda\overline{\Lambda}$ Formation in Two-Photon Collisions at LEP

The L3 Collaboration

Abstract

The reaction $e^+e^- \rightarrow e^+e^-\Lambda\overline{\Lambda}$ X is studied with the L3 detector at Lep using data collected at center of mass energies from 91 GeV to 202 GeV, for an integrated luminosity of 616 pb^{-1}. The cross section is compared to quark-diquark model predictions.

Submitted to the
XXXth International Conference on High Energy Physics
Osaka, Japan, July 27 - August 2, 2000.

1 Introduction

The electron-positron storage rings are, at present, the only available accelerators for the study of two-photon interactions, via the process $e^+e^- \rightarrow e^+e^-\gamma^*\gamma^* \rightarrow e^+e^-X$, where γ^* is a virtual photon. The outgoing electron and positron carry nearly the full beam energy and their transverse momenta are usually small, so they are not detected. The system X has therefore a low mass value with respect to the e^+e^- center of mass energy.

The photon flux is calculable by QED [1] and the reaction $\gamma^*\gamma^* \rightarrow$ hadrons is useful to study the strong interactions. Using the Brodsky-Lepage hard scattering approach [2], predictions have been made for the production of baryons in two-photon interactions. The CLEO measurement [3] of the $\gamma\gamma \rightarrow p\overline{p}$ cross section is inconsistent with the prediction of a pure quark model [4]. A quark-diquark model [5], which takes into account non-perturbative quark-quark correlations inside baryons, reproduces rather well the $p\overline{p}$ data, but the cross section measurement of $\gamma\gamma \rightarrow \Lambda\overline{\Lambda}$ [6] is higher than the value predicted by the model.

In this paper we present the first analysis of $\Lambda\overline{\Lambda}$ production at Lep, using data collected by the L3 detector. The results are preliminary. In this analysis the Σ^0 is not identified thus the cross section measurement refer to the channel $\gamma\gamma \rightarrow (\Lambda/\Sigma^0)\,(\overline{\Lambda}/\overline{\Sigma}^0)$.

2 The detector and the Monte Carlo

A detailed description of each subsystem of the L3 detector and its performance is given [7] and [8]. The analysis described in this paper is based on the central tracking system and on the high resolution electromagnetic calorimeter. The events are collected predominantly by the track triggers [9].

The events are simulated by the EGPC Monte Carlo [10]. For each experimental energy a sample of events [1)] was generated with the luminosity function of transverse photons. The $\gamma\gamma$ mass is generated constant from the $\Lambda\overline{\Lambda}$ threshold to 5 GeV. Its decay into $\Lambda\overline{\Lambda}$ is generated uniformly in the $\gamma\gamma$ center of mass. The events were simulated in the L3 detector using GEANT [11] and GEISHA [12] programs and passed through the same reconstruction program as the data.

3 Event selection

To analyse the reaction $e^+e^- \rightarrow e^+e^-\Lambda\overline{\Lambda}$ X, only the $\Lambda \rightarrow p\pi^-$ and $\overline{\Lambda} \rightarrow \overline{p}\pi^+$ decays are considered.

The selection of events is as follows:

- There must be exactly four good charged tracks in the tracking chamber with a net charge of zero. A good track requires more than 12 hits out of a maximum of 62.
- There must be two secondary vertices with a distance greater than 3 mm in the transverse plane from the primary interaction vertex.
- The angle between the flight direction of each Λ candidate (taken as the line between the interaction vertex and the secondary vertex in the transverse plane) and the total transverse momentum vector of the two outgoing tracks must be smaller than 0.15 rad.

[1)] The statistics of each sample is at least ten times bigger than the data

- At each decay vertex, the p and $\overline{\mathrm{p}}$ are identified as the track with the largest momentum. They must have opposite charge.

- If a secondary vertex is due to a photon conversion, the event is rejected. A conversion is recognized by assigning the electron mass to the two tracks and a cut $M_{e^+e^-} > 0.05$ GeV is applied.

- For each particle, p or π, the dE/dx measurement must be inside a band of $\pm$ 45% around the nominal value (see Fig.1).

- Often the antiproton annihilates in the electromagnetic calorimeter. It is identified by requiring that the electromagnetic energy, associated to the track, be above the value: $E_{em} > 0.35$ GeV. This cut removes 30

- To suppress the K^0_S background, we use the Podolanski-Armenteros variables [13]. In the plane of the transverse (P_T) vs the longitudinal (P_L) component of the positive particle momentum, relative to the momentum vector of the neutral particle (P_n), the K^0_S and the Λ are caracterized by very distinct ellipses (Fig.3). The cuts $P_T < 0.13$ GeV and $|(P_L/p_n) - 0.5| > 0.1$ remove most of the $K^0_S K^0_S$ background.

- To compare with theoretical predictions a cut $|\cos(\theta^*)| < 0.6$ is applied, where θ^* is the polar angle in the two-photon center of mass system, taking the z direction parallel to the electron beam. This cut removes very few events, since the detector acceptance is almost limited to this angular range.

No rejection is applied to events which have photons or a large missing transverse momentum. After these cuts 159 events are selected.

The two-dimensional plot of the $p\pi^-$ mass vs the $\overline{p}\pi^+$ mass is shown if Fig.4, where a clean $\Lambda\overline{\Lambda}$ signal is present. The Λ and the $\overline{\Lambda}$ are at the nominal value [14] and the mass resolution is compatible with the Monte Carlo expectation (σ = 6 MeV). The $\Lambda\overline{\Lambda}$ events are then selected within a radius of 40 MeV around the value of 1.115 GeV. The number of events for the different center of mass energies are listed in Table 1. A typical event is shown in Fig. 5.

The effective mass distribution of the $\Lambda\overline{\Lambda}$ system is shown in Fig.6 for the 44 events selected. The $K^0_S K^0_S$ background, shown in Fig.6, is evaluated with the corresponding $K^0_S K^0_S$ data sample [15]; it is estimated to be 4.2 events.

4 Results

The detector acceptance and efficiency is calculated by Monte Carlo, taking into account the experimental conditions of each year of data taking (Table 1). From the selected $\Lambda\overline{\Lambda}$ events, estimated after substraction of the background, we obtain a cross section

$$\sigma(e^+e^- \to e^+e^-(\Lambda/\Sigma^0)(\overline{\Lambda}/\overline{\Sigma}^0)) = 4.13 \pm o.65 \text{ (stat.)} \pm 0.69 \text{ (syst.) pb.}$$

The systematic error is evaluated by considering the uncertainty on the selection cuts, the efficiency corrections, the background substraction and the two-photon luminosity function. The individual contributions are listed in Table 2.

Deconvoluting the two-photon luminosity function and extrapolating the measurement that correspond to the interaction of real photons [16], we extract the cross section $\sigma(\gamma\gamma \to (\Lambda/\Sigma^0)(\overline{\Lambda}/\overline{\Sigma}^0))$ shown in Fig.7. In Fig.7a) our measurement is compared to the one obtained by CLEO [6]. Although the results are compatible inside large experimental errors, the mass dependance of

CLEO is steeper than the one we observe. A fit to our data of the form $\sigma \propto \mathrm{M}^{-\mathrm{n}}$ gives a value $\mathrm{n} = 8.69 \pm 3.81$ while a similar fit to CLEO gives $\mathrm{n} = 16.06 \pm 5.78$ (Fig. 7b).

In Fig.7c) our data are compared to the expectations of the recent calculations of C.Berger, B.Lechner and W.Schweiger [17]. In their diquark model they consider three different distribution amplitudes for the octet baryons (DA in the Fig.7c). Our data lie above the predictions, as expected because of the Σ^0 contamination included in the selection, but the observed mass dependance is rather well reproduced.

This is the first measurement at LEP of dibaryon production in two-photon interactions; this analysis will be extended to other baryons in the near future.

5 Acknowledgments

We thank C.Berger and W.Schweiger for very useful discussions and providing us their theoretical predictions.

References

[1] V.M.Budnev *et al., Phys. Rep.* **C 15** (1975) 181.

[2] S.J.Brodsky et J.P.Lepage, *Phys. Rev.* **D 22** (1980) 2157.

[3] CLEO collaboration, M.Artuso *et al., Phys. rev.* **D 50** (1994) 5484.

[4] G.Farrar *et al., Nucl. Phys.* **B 259** (1985) 702; *Nucl. Phys.* **B 263** (1986) 746(E).

[5] M.Anselmino, F.Caruso, P.Kroll et W.Schweiger, *Int. J. Mod. Phys.* **A 4** (1989) 5213.

[6] CLEO collaboration, S.Anderson *et al., Phys. Rev.* **D 56** (1997) R2485.

[7] L3 Collab., B.Adeva *et al., Nucl. Instr. Meth.* **A 289** (1990) 35.

[8] M.Acciarri *et al., Nucl. Instr. Meth.* **A 351** (1994) 300.

[9] P.Béné *et al., Nucl. Inst. Meth.* **A 306** (1991) 150;
D.Haas *et al., Nucl. Inst. Meth.* **A 420** (1991) 101.

[10] F.L.Linde, "Charm Production in Two-Photon Collisions", Ph.D. Thesis, Rijksuniversiteit Leiden, 1988.

[11] R.Brun *et al.*, GEANT 3.15 preprint CERN DD/EE/84-1 (Revised 1987).

[12] H.Fesefeldt, RWTH Aachen report PITHA 85/2, 1985.

[13] J.Podolanski et R.Armenteros, *Phil. Mag.***45** (1954) 13.

[14] Particle Data Group, C.Caso *et al., Eur. Phys. J.* **C 3** (1998) 1.

[15] L3 collaboration, '$\mathrm{K^0_S K^0_S}$ Final State in Two-Photon Collisions and Glueball Searches', L3 note 2557 submitted to this Conference.

[16] G.A.Schuler, Improving the equivalent-photon approximation in electron-positron collisions, hep-ph/9610406, CERN-TH/96-297.

[17] C.Berger, B.Lechner and W.Schweiger, *Fizika* **B 8** (1999) 371 hep-ph/9901338.

$\sqrt{s}$ GeV	Luminosity pb^{-1}	Events	Efficiency %
91	147.	15	1.80 ± 0.11
183	61.	3	1.42 ± 0.11
189	175.	9	1.42 ± 0.08
192-202	233.	17	1.47 ± 0.08

Table 1: The number of $\Lambda\overline{\Lambda}$ events for each energy sample. The integrated luminosity and the measured efficiency is also given.

Sources of systematic errors	Uncertainty %
dE/dx cut	101.
$\overline{p}$ e.m. energy cut	10.3
$\lvert\cos(\theta^*)\rvert$ cut	3.7
Λ definition	2.2
efficiency	4.1
$K^0_S K^0_S$ background	4.3
two-photon luminosity function	4.6
Total	16.8

Table 2: Evaluation of the systematic errors

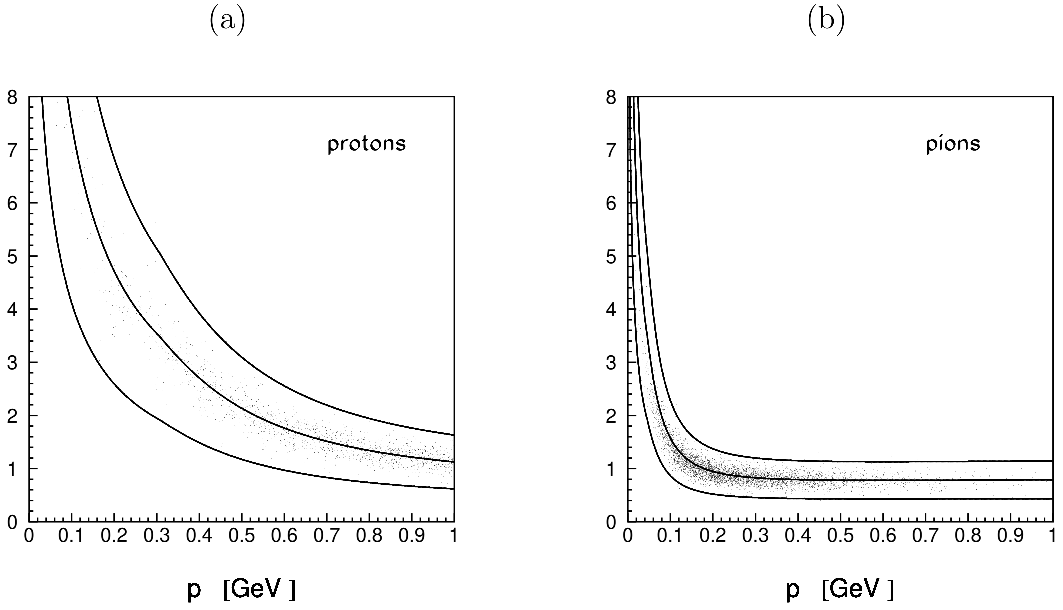

Figure 1: dE/dx measurement as a function of the particle momentum of a) protons b) pions from the Monte Carlo simulation. The central value and the accepted band of ±45% are indicated.

(a) (b)

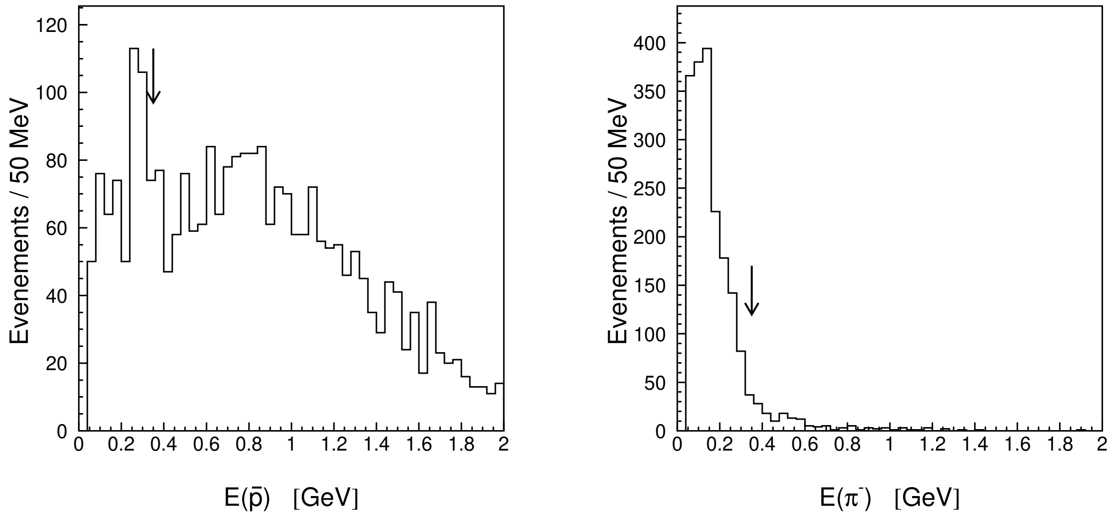

Figure 2: Energy deposited in the electromagnetic calorimeter by a) $\overline{p}$ and b) π^- from Monte Carlo.

(a) (b)

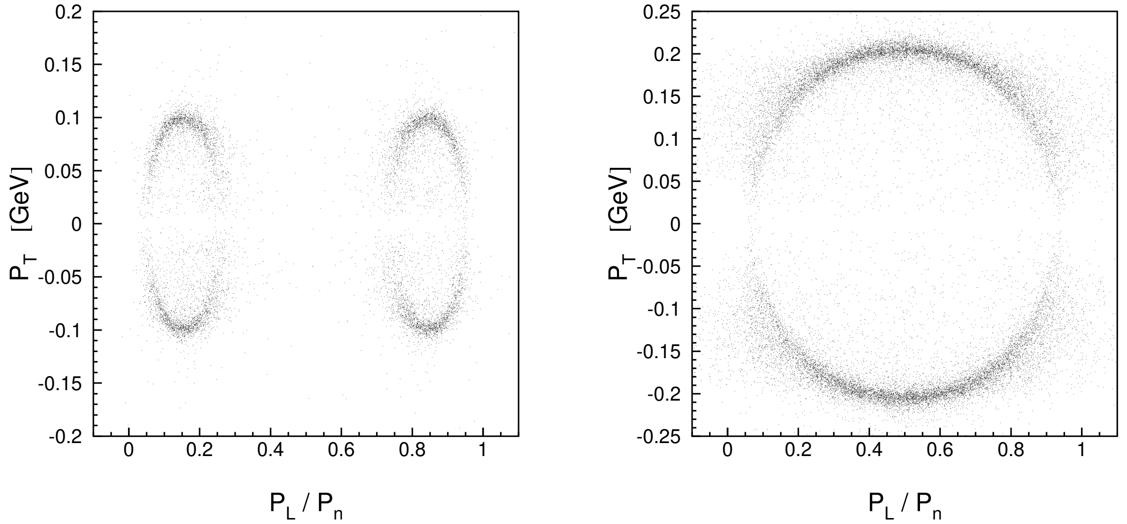

Figure 3: The Podolanski-Armenteros plot of transverse ($\mathrm{p_T}$) vs the longitudinal ($\mathrm{p_L}$) component of the positive particle momentum, relative to the momentum vector of the neutral particle ($\mathrm{p_n}$). Distribution for a) Λ and b) $\mathrm{K^0_S}$ from Monte Carlo simulation. The cuts $\mathrm{p_T} < 0.13$ GeV and $|(\mathrm{p_L}/\mathrm{p_n}) - 0.5| > 0.1$ remove most of the $\mathrm{K^0_S}$ background.

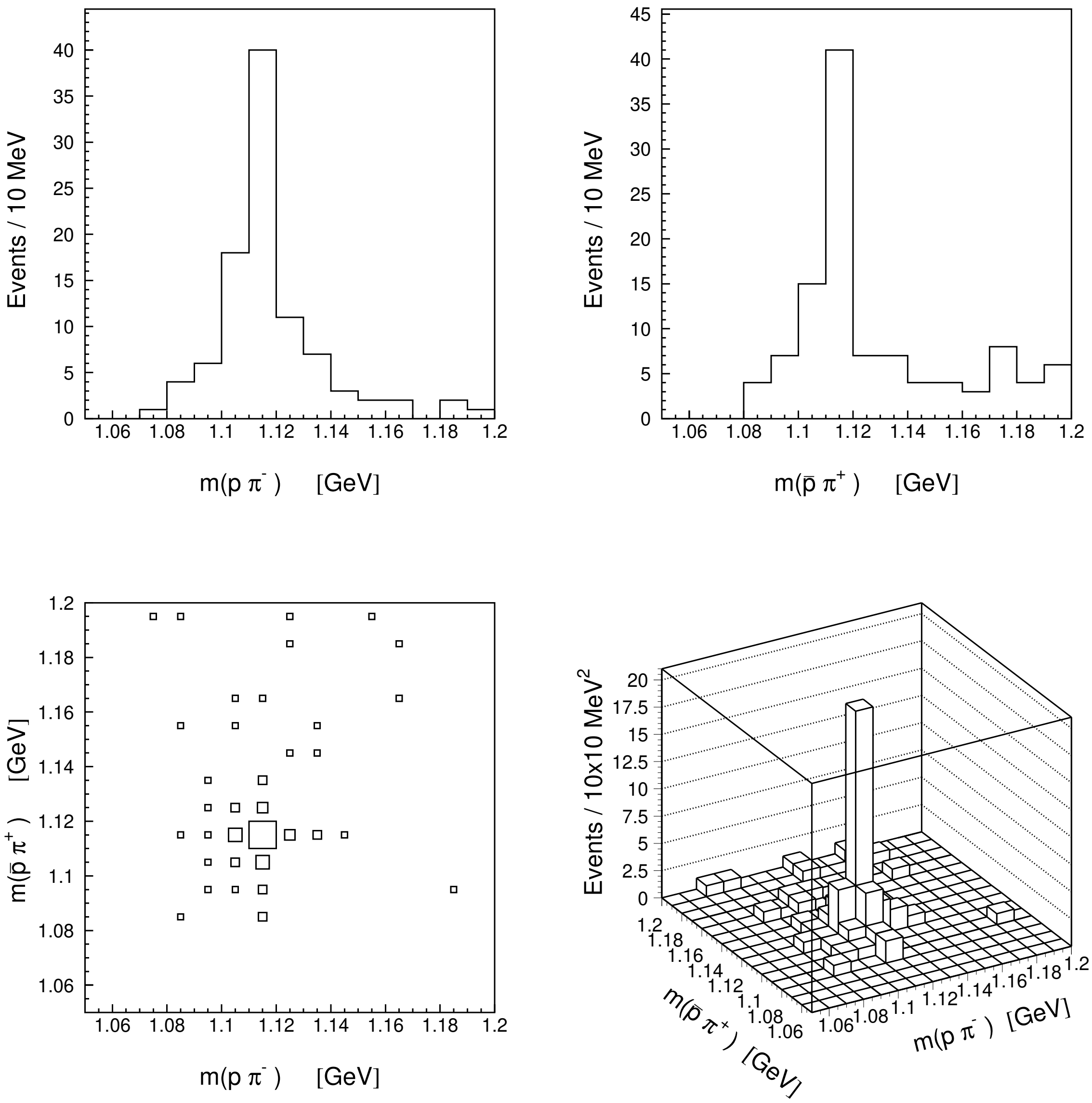

Figure 4: The distributions of $\mathrm{p}\pi^-(\Lambda)$ and $\overline{\mathrm{p}}\pi^+(\overline{\Lambda})$ for the selected events. A radius of 40 MeV around the nominal mass value of Λ in the two-dimensional plot defines the $\Lambda\overline{\Lambda}$ sample.

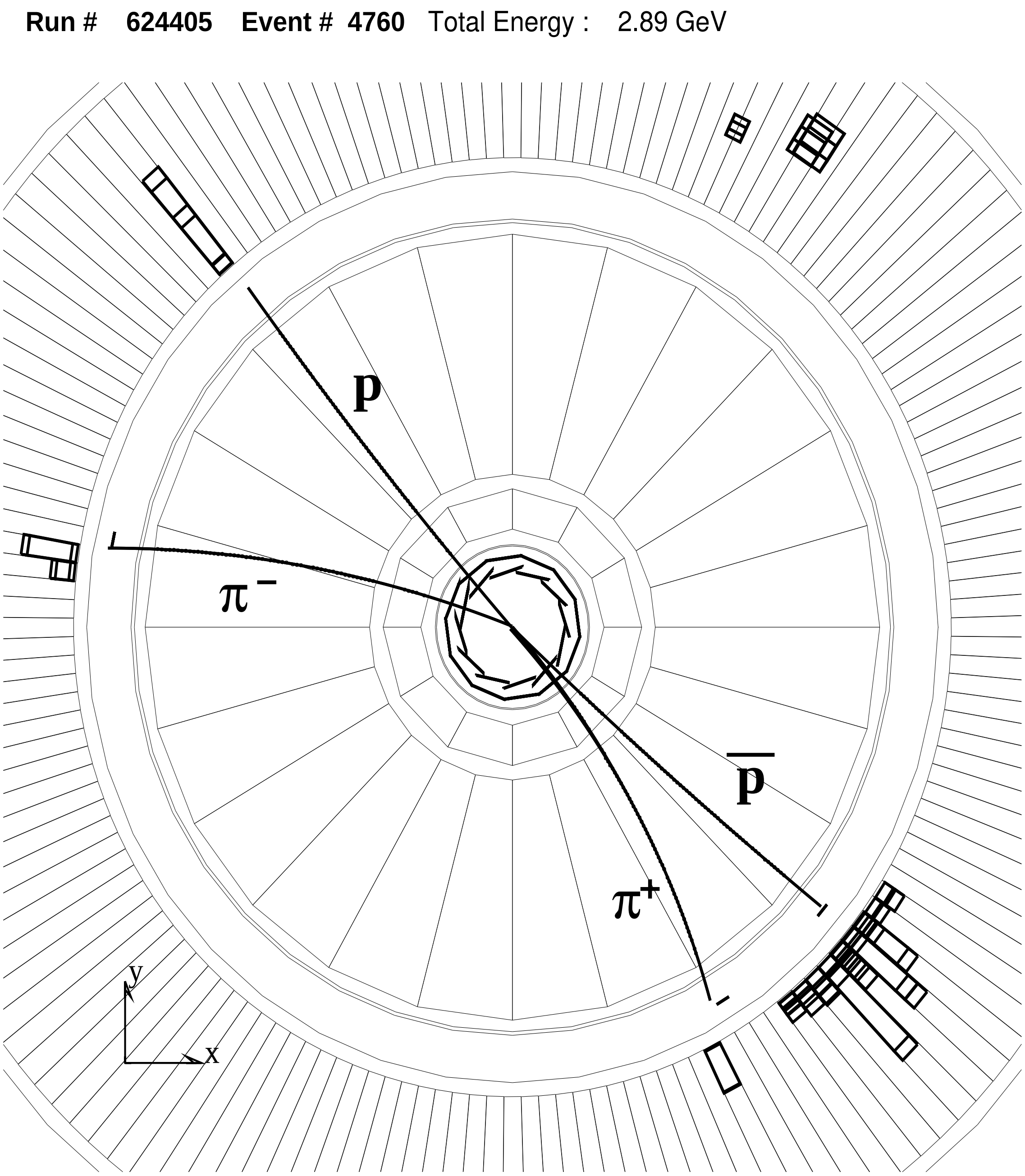

Transverse Imbalance :	.3103	**Longitudinal Imbalance :**	.1273
Thrust : .7656	**Major :** .4285	**Minor :** .1385	
Event DAQ Time :	*941112 200904*		

Figure 5: A selected event, displayed in the transverse plane.

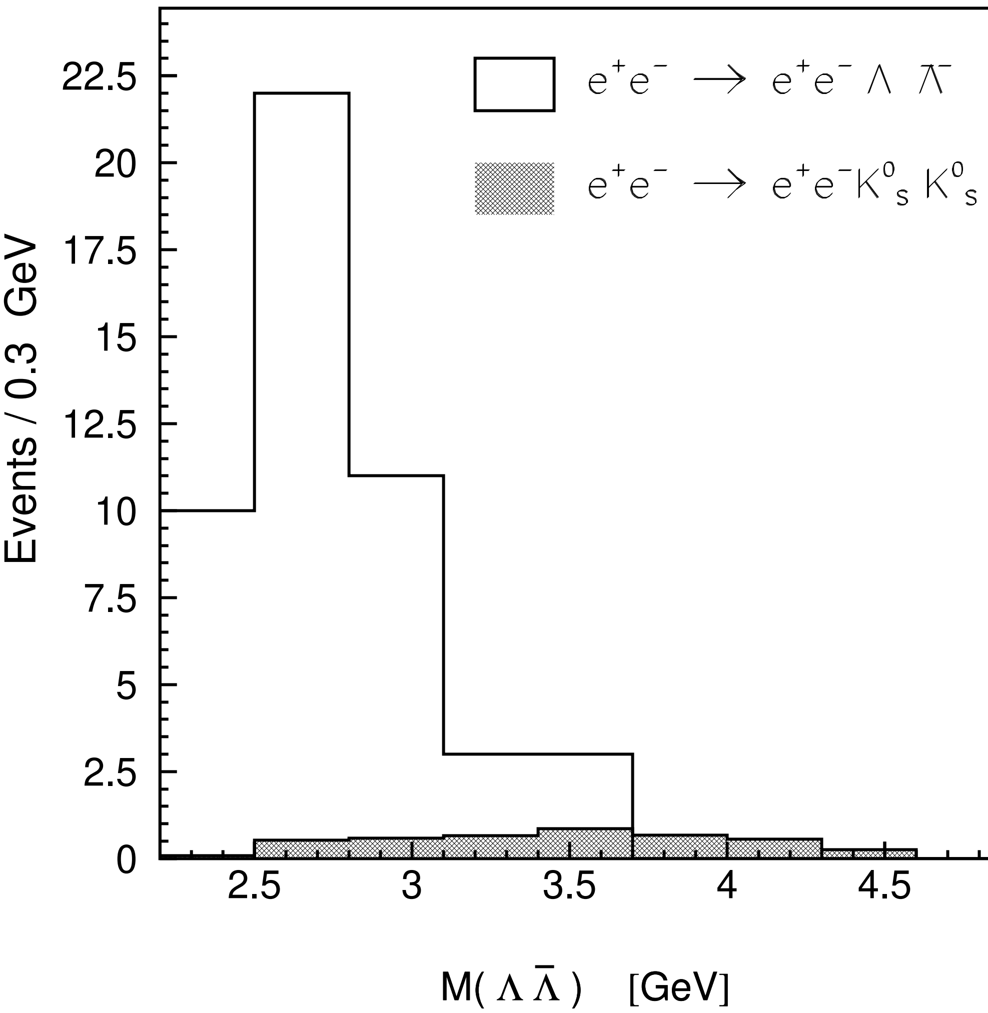

Figure 6: The $\Lambda\overline{\Lambda}$ mass spectrum of the selected events. The $K^0_S K^0_S$ background is indicated as a shaded histogram.

(a)

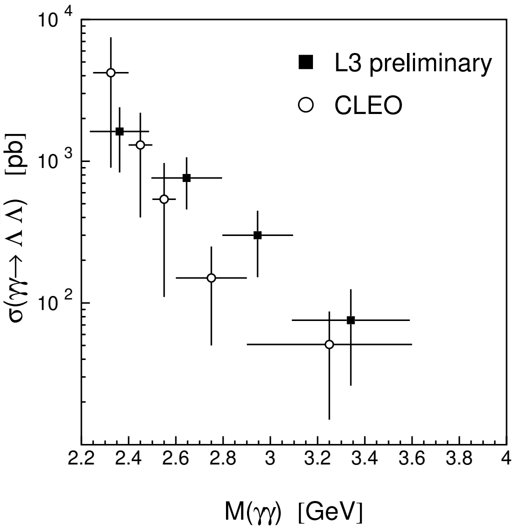

(b)

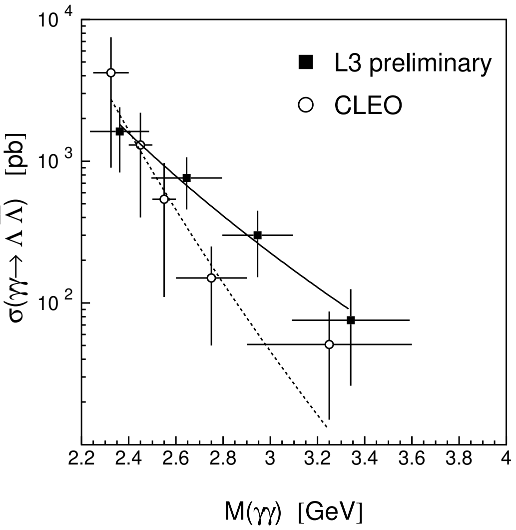

(c)

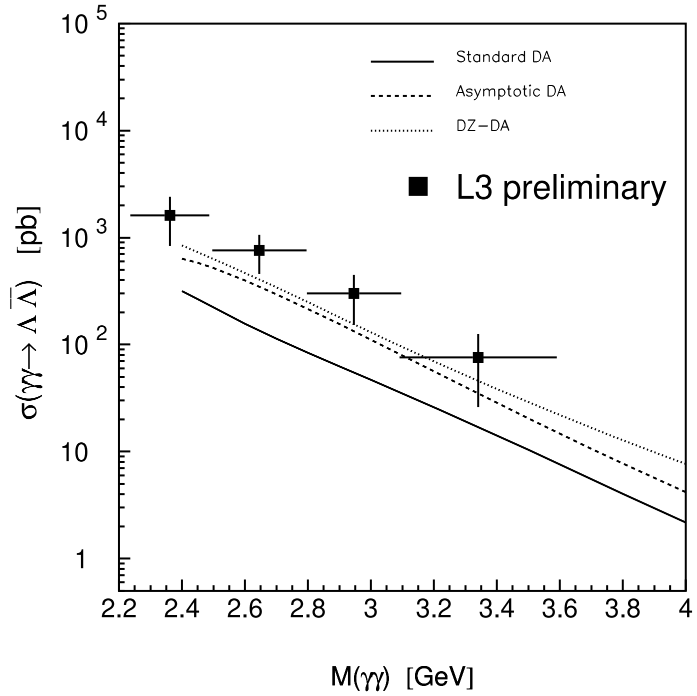

Figure 7: The measured cross section $\sigma(\gamma\gamma \rightarrow (\Lambda/\Sigma^0)(\overline{\Lambda\Sigma}^0))$ a) compared to CLEO [6] b) the same as a) with the fits described in text superimposed c) compared to the calculations of ref.[17].